

Designing an Experiment to Measure H_2^+ production in IsoDAR's Multicusp Ion Source

Román Via-Dufresne Saus

under the direction of

Joseph Smolsky

Department of Nuclear Science
Massachusetts Institute of Technology

Research Science Institute
July 31, 2018

Abstract

In this paper it is described the designing process of an experiment to test a multicusp ion source H_2^+ production. This ion source will be used in the Isotope Decay At Rest (IsoDAR) experiment, which has the goal of producing and analyzing neutrinos to prove the sterile neutrinos' existence. To measure H_2^+ , the ion beam will be directed to an emittance sensor along a Low Energy Beam Transport (LEBT) system with two quadrupole magnets and one dipole one. This project explains how different configurations - changing the magnets order and the magnetic fields applied - were computationally simulated and evaluated. It has been found that the best configuration consists in placing the dipole magnet between the quadrupoles. The magnetic fields to be applied cannot be determined due to the impossibility to know the space charge compensation in the LEBT.

Summary

In this paper, an experiment to test an ion source efficiency is designed. This ion source will be used in the Isotope Decay At Rest (IsoDAR) experiment, which is being created to determine if sterile neutrinos exist. To measure the ion source's efficiency, the ions will be directed to a scanner using two quadrupole (four poles) magnets and one dipole (two poles) one. To find the best configuration, some computational simulations have been run. We found that the best option is to place the dipole magnet between the quadrupoles. Their magnetic fields cannot be found due to an unpredictable essential value.

1 Introduction

The multicusp ion source is an essential part of the IsoDAR experiment, which is being created to prove the existence of the sterile neutrino. This ion source is already built but needs to be tested and optimized. To do so, we will measure H_2^+ production using a Low Energy Beam Transportation System, which we will design and improve through simulations.

1.1 Isotope Decay At Rest (IsoDAR)

The sterile neutrino is a theoretical particle whose existence has not been proved yet. It was proposed as a result of many recent neutrino oscillation experiment, such as LNSD[1], KATRIN[2] or MiniBooNE[3], which found some anomalies that did not match the Standard Model; some of them with a 4σ uncertainty. The sterile neutrino should only interact with the gravitational force, so it cannot be detected. Therefore, the only way to prove its existence is by studying the other types of neutrinos. None of the experiments performed until this moment have shown enough reliable results to be able to prove the sterile neutrino's existence. The goal of the Isotope Decay At Rest (IsoDAR) experiment is to prove the sterile neutrino's existence with a 5σ uncertainty.

IsoDAR will study neutrinos by producing and analyzing them in the same experiment. Electron antineutrinos ($\bar{\nu}_e$) will be used. In the very beginning of the neutrino production process, a proton source is required. To obtain the necessary amount of $\bar{\nu}_e$, 10mA of cyclotron-accelerated p^+ is needed[4].

Instead of directly producing protons, H_2^+ will be used. Using H_2^+ will ease the cyclotron acceleration system, because the beam will be more compact and easier to drive. As H_2^+ is formed by one electron that couples two protons, the cohesion of the charges will be much better. Moreover, only 5mA of H_2^+ will have to be produced. After getting accelerated in the cyclotron, a carbon stripper will knock out the electron and the final 10mA of protons will

be obtained.

1.2 Multicusp Ion Source Technology

IsoDAR will be using a Multicusp Ion Source Technology (MIST) to produce H_2^+ . MIST is based on a similar source developed by the Lawrence Berkeley National Lab in the 1980s[5], though that one was developed for other purposes.

MIST is a plasma, filament-driven, multicusp ion source. H_2 is confined in the plasma chamber and some current flows through the filament. A voltage difference is applied between the filament and the MIST front plate and electrons are expelled from the filament. When the electrons hit H_2 molecules, they ionize and plasma forms. To confine the plasma and the electrons, a multicusp magnet field is used, shown in Figure 1.

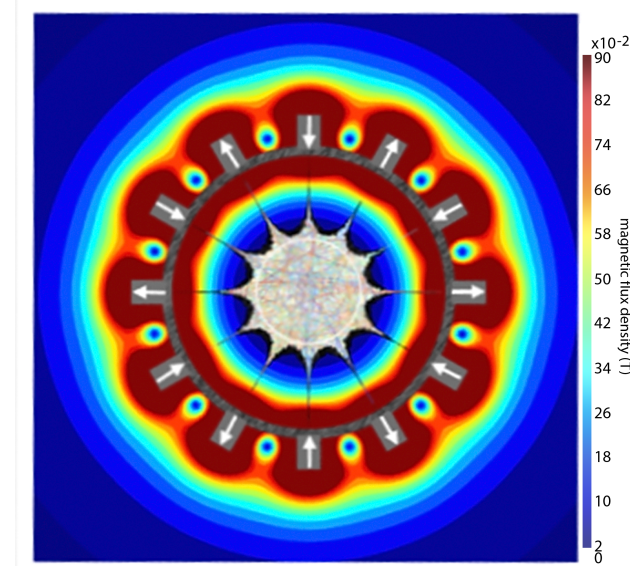


Figure 1: MIST's multicusp magnetic field simulation. The magnetic flux density is color-mapped from dark red (0.9 T) to dark blue (0.02 T). The color bar shows the value of each color in $T \times 10^{-2}$.

12 radial custom designed samarium cobalt magnets (Sm_2Co_17), plus 6 more in the front

plate are used to create the multicusp magnetic field. Sm_2Co_17 is used instead of other rare earth magnets so that the plasma chamber can operate at a higher temperature, allowing higher ion current density. A tungsten filament is used, with an expected lifetime between 30 and 100h.

The extraction system consists of two puller electrodes with different voltage potentials and a focusing lens with three different parts with individual potentials. This system pulls the particles through the extraction hole and gives the beam its initial shape and acceleration.

While MIST has already been designed and built, there are some parameters that can still be adjusted to improve its performance. These parameters include filament current, voltage, shape and thickness, extraction hole size, lens and puller voltages and pressure in the plasma chamber. The filament parameters the pressure affect the H_2^+ production, while the other parameters affect its extraction. MIST has been designed to be modular, so it is easy to change all these parameters.

1.3 Low Energy Beam Transportation

To test the MIST efficiency, we will design an experiment to measure the H_2^+ produced. We need to measure exclusively H_2^+ , even though, there are many other subproduct particles extracted from it. Although we currently have methods to measure the total current extracted from the MIST, we can only approximate how much is due to H_2^+ . Therefore, we need a method to filter H_2^+ from the other particles to measure it separately. Moreover, we need to transmit as much H_2^+ as possible to the sensor to know the true quantity.

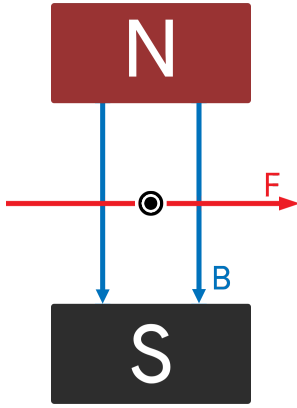


Figure 2: Dipole magnet diagram. The rectangles represent the magnetic poles. The central dot represents the beam (exiting the page). Blue lines represent the magnetic field direction. Red lines represent the force direction exerted on the beam.

To do so, we will use a Low Energy Beam Transport (LEBT) with a dipole electromagnet (Fig. 2) and two quadrupoles (Fig. 5) to drive H_2^+ to an emittance scanner (described in section 6). Three different layouts have been proposed: a dipole-quadrupole (qd), a dipole-quadrupole-quadrupole (dqq) and a quadrupole-dipole-quadrupole (dqd). These names refer to the order in which the magnets would be arranged following the beam direction, as Figure 3 shows. Notice that in the first proposed layout we are just using one of the two quadrupole magnets.

The dipole electromagnet will work as a particle filter. Neutral particles will not be affected by the magnet and will continue their straight path, not reaching the sensor. Charged particles will bend depending on their charge and their mass.

The magnetic field will bend particles with different charges in different ways. Therefore only particles with +1 charge will be affected in the same way as H_2^+ . But even if some particles have the same charge as H_2^+ , for example p^+ , they will not have the same mass as H_2^+ and they will follow a different path. A particle's path can be calculated from Equation

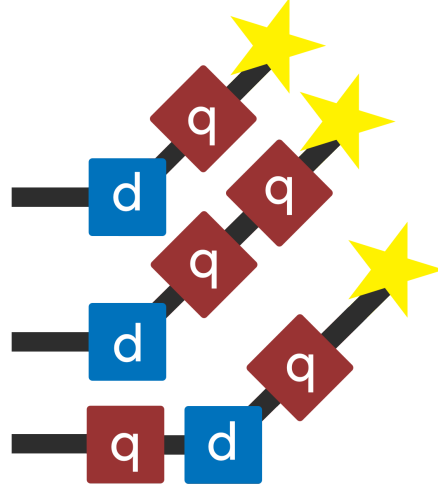


Figure 3: Simplified schematics of the three layouts proposed for the LEBT: dq, dqq and qdq from top to bottom. Black lines represent the paths followed by the beam. Blue squares represent dipole magnets. Red squares represent quadrupole magnets. Stars represent the sensor.

1:

$$m \frac{v^2}{r} = qB, \quad (1)$$

which equates the centripetal force to the magnetic force, that will be equal all along the path the beam follows. From Equation 1 we can obtain the equation

$$r = \frac{mv^2}{qB}, \quad (2)$$

where is shown how the radius (r) of the path the particles will follow depends on their mass (m), their velocity (v) and their charge (q). The magnetic field (B) will affect them all equally. Particles with less mass and more charge will be more bent. Moreover, velocity is the same for all particles and will not affect their bend.

Although it is possible to calculate the required magnetic field using the expression

$$B = \frac{mv^2}{qr}, \quad (3)$$

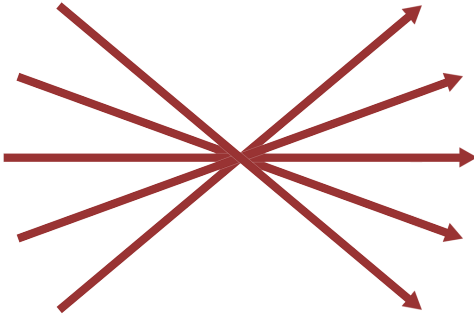


Figure 4: Converging beam becoming diverging. Arrows represent the path followed by different particles in the beam.

we do not know all the dipole specifications nor the current needed. Therefore, the current will be adjusted manually once the experiment is mounted.

The quadrupole electromagnets will help to drive and shape the beam to avoid particle loss. The transmission of the particles will depend on their magnetic fields. The quadrupoles will have to maintain a non convergent nor divergent beam of $< 5\text{cm}$ diameter to ensure that as many particles as possible reach the sensor. A longer beam diameter means that particles are very separated, and they may spread out, exit the path, and get lost. If the beam is divergent, particles are spreading out and will end up getting lost. If it is convergent, it will eventually be divergent (Figure 4) and the same will happen.

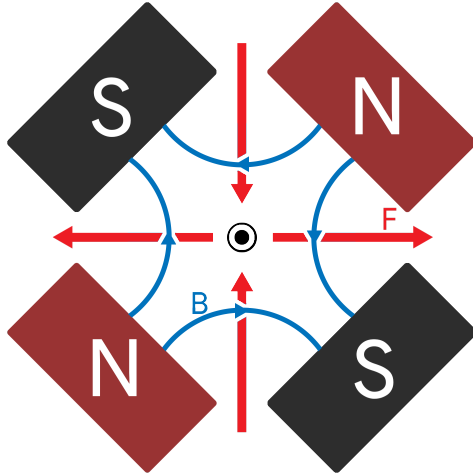


Figure 5: Quadrupole magnet diagram. Rectangles represent magnetic poles. The central dot represents the beam (coming in our direction). Blue lines represent the magnetic field direction. Red lines represent the force direction exerted to the beam.

Notice that quadrupole magnets have an opposite effect in perpendicular directions, as can be observed in Figure 5. All the qualities mentioned in the paragraph above have to apply to both x and y dimensions of the beam.

2 Methods

To find the optimal configuration of the LEBT, we have run WARP simulations with different values for the key parameters that affect the beam transmission and shape.

2.1 Parameters

The different possible configurations of the LEBT depend on four parameters: magnet order, charge compensation, the magnetic field of the first quadrupole magnet and the magnetic field of the second one.

The beam will be affected by the order in which we arrange the magnets and, as explained in Section 1.3, three different layouts have been proposed: dq, dqq, qdq.

Another parameter is space charge compensation, due to the fact that the beam is formed by many same-sign charged particles traveling in proximity to each other. All the individual positive charges (H_2^+) can collectively be considered as a space charge, which will cause the particles to spread out by repulsion. However, the vacuum applied in the LEBT will not be perfect and there will be some gases. Most of the particles forming these gases do not have positive charge and some of them even have negative charge. For this reason, space charge will be partially compensated and dissipated by the remaining gases in the LEBT. This phenomenon is called space charge compensation ($q\ comp$) and its value is calculated as follows:

$$q\ comp = \frac{\text{dissipated space charge}}{\text{initial space charge}}. \quad (4)$$

Space charge compensation is a value that we cannot control nor measure. Our vacuum system is not good enough to produce a specific charge compensation and we do not dispose of a way of measuring it. However, this value can greatly affect the behavior of the beam. For this reason, we have performed each simulation with three different values: 0, 0.5 and 0.8 charge compensation. This way it will be easier for us to adapt to the real situation. We expect to have a value between 0.5 and 0.8 in the real experiment.

The final values are the magnetic fields of the quadrupole magnets. We will only adjust the fields for the quadrupole magnets because the dipole magnet field has to be the specific field that sorts H_2^+ from other particles. In the dq simulations, we will only adjust one magnetic field value, as it only uses one quadrupole magnet. In the dqq case, the fields will have opposite sign because, as explained in Section 1.3, quadrupole magnets affect the x and y dimensions of the beam in opposite ways. This way, one quadrupole will compensate for the other. In the qdq layout, both quadrupole field values will have the same sign because

the dipole magnet unfocuses more one dimension than the other, and we use the quadrupole fields to compensate for it.

2.2 Simulations

Simulations have been run with a Python3 script that uses the WARP module. WARP is an open-source Python package designed for particle-in-cell simulations of plasmas and high current particle beams [6]. These simulations have been run for each layout testing different magnetic fields for the quadrupole magnets to try to find which configuration obtained optimum transmission and beam shape. Each simulation has also been run with the three qcomp values: 0, 0.5 and 0.8. The simulations work as follows:

The initial positions and velocities of the particles are obtained from a simulation of the extraction system of the MIST carried out by the graduate student Loyd Waites using IBSimu[7]. With this data and the physical dimensions of the LEBT parts, the WARP script calculates the position and velocity of each particle frame by frame (in our case with a step size of 1mm). In each frame, it generates a 2D grid (we use one of 256x256) in which locates the particles. Knowing each particles' location and velocity, and the forces exerted on them by the magnetic fields and among the particles due to their charge, the program calculates the new values for the next frame. This procedure is repeated until the end of the simulation.

Once the WARP simulations end, the main Python3 generates figures showing the beam size along the LEBT and the final shape (see section 3).

To run the simulations an iterator script has been used to ease the process. The iterator script can run the main script several times changing the input values each time. Even though, the process has not been totally automated. Although the code could have been easily edited to analyze the transmission obtained, it would be harder to computationally analyze the shape of the beam, as it is not just a numerical value. Therefore, the values that the iterator script used have been manually input as a list and then run.

3 Results

Top Transmission Configurations				
Order	q Comp.	B1 (T)	B2 (T)	Transmission (%)
dq	0.0	-0.07	-	37.4
	0.5	-0.25	-	76.5
	0.8	-0.12	-	98.4
dqq	0.0	-0.24	0.24	28.3
	0.5	-0.24	0.24	70.6
	0.8	-0.25	0.15	98.5
qdq	0.0	-0.41	-0.06	40.6
	0.5	-0.27	-0.09	68.4
	0.8	-0.17	-0.11	99.0

Table 1: Top transmissions obtained with the simulations with different configurations. The columns display the order of the magnets, the charge compensation and the magnetic fields used for the first and the second quadrupole magnets.

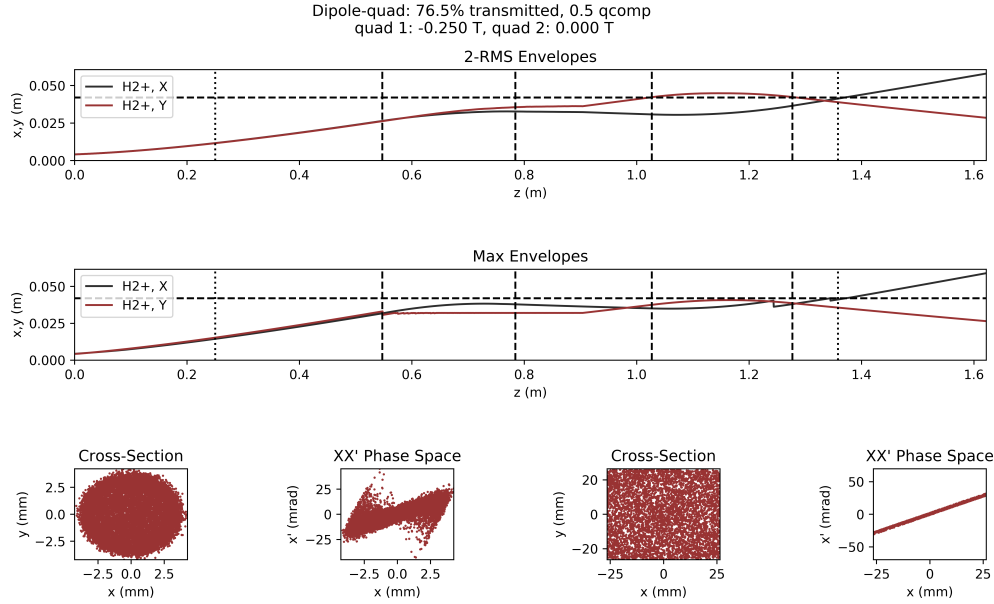


Figure 6: Top transmission result obtained from the dq simulations with a qcomp value of 0.5.

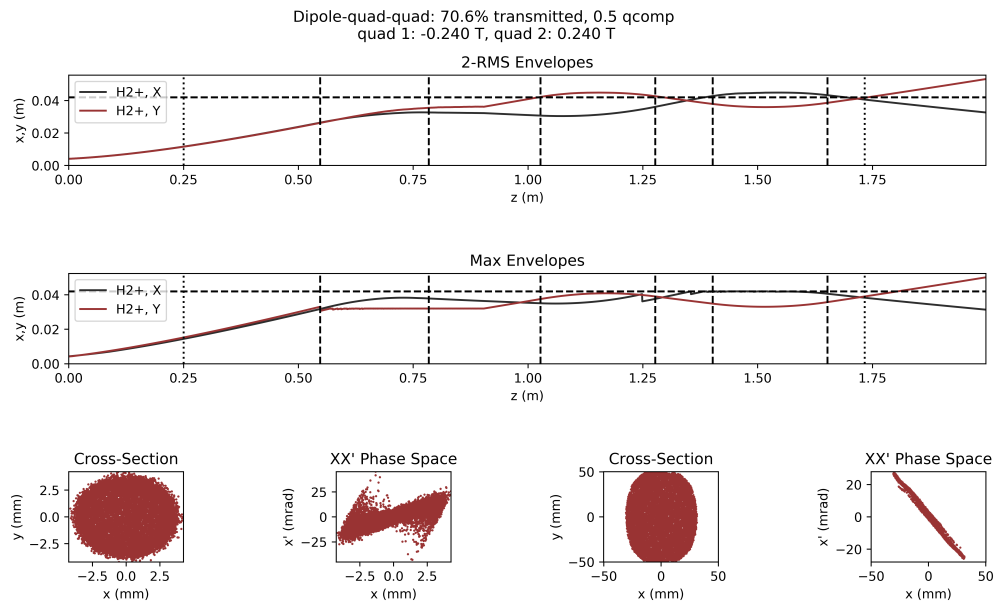


Figure 7: Top transmission result obtained from the dqq simulations with a qcomp value of 0.5.

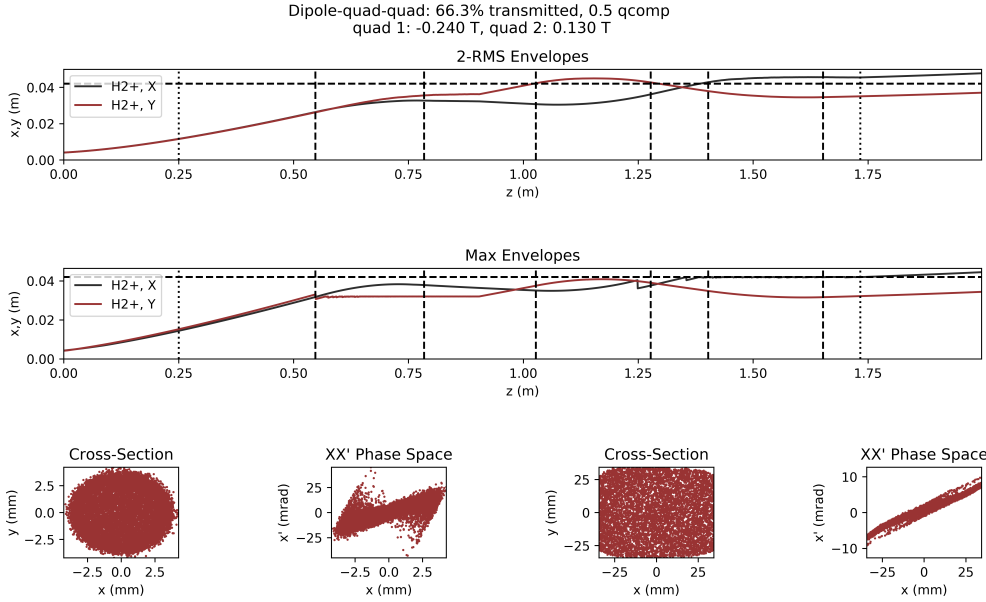


Figure 8: Better shape result obtained from the dqq simulations with a qcomp value of 0.5.

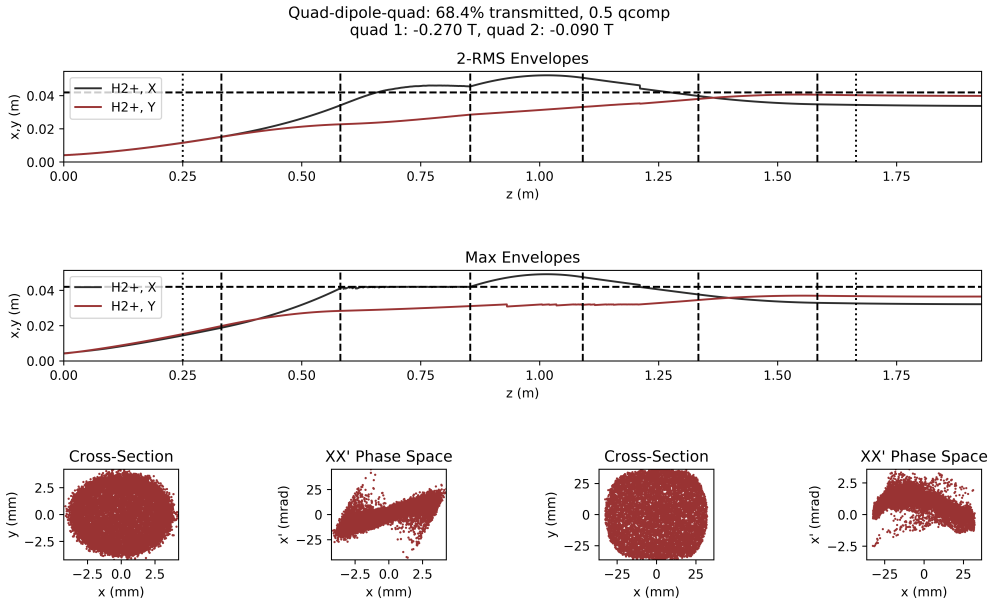


Figure 9: Top transmission result obtained from the qdq simulations with a qcomp value of 0.5.

The magnetic field configurations for each layout and charge compensation that obtained the highest transmission are shown in Table 3. Figures 6 to 9 show the best results obtained for each layout with 0.5 qcomp. Best results with other charge compensation values can be consulted in the Appendix.

The figures obtained with the Python3 script module contain six different plots. *2-RMS Envelopes* and *Max Envelopes* show the size of the beam of both x and y dimensions along the entire LEBT length. The former shows the average root mean square[8] size of the beam and the latter shows the maximum size. The first plot is especially useful because the maximum width of the beam can change by just one single deviated particle. Optimal-shaped beams have near zero slope for both x and y at the end of the LEBT because positive slope plots show divergent beams and negative slope plots are convergent beams.

There are two pairs of plots at the bottom of each figure: initial and final plots. The left plot of each pair shows the (x, y) position of each particle, so the shape of the beam can be intuitively observed. The right plot of each pair shows a plot of the velocity in the x direction (x') of the particles along the x position axes, so we can see if the beam's size is changing. Therefore, an optimal beam will have all particles near zero on the y axis. This means that the beam is not divergent nor convergent. We are only interested in the right pair of plots (final plots). The plots from the left side show the initial data, which is the same for all results and is referential.

Some characteristics of each layout were also found while running the simulations. The qd simulations were the easiest to run, as only one magnetic field had to be found.

The dqq optimization was the most difficult, as both fields affect both the transmission and the shape of the beam. Therefore, there was not an algorithm we could use to find the optimal transmission and shape. A lot of simulations had to be run due to the great amount of possible magnetic fields combinations.

In the case of qdq, it was found that the field of the first magnet mainly affected the

transmission and the second one affected the shape. The entrance to the dipole is the part of the LEBT in which a larger number of particles can be lost. Therefore, the path that the beam follows before reaching the dipole - regulated by the first quadrupole magnetic field - affects the transmission. Instead, the other magnet's field does not substantially affect the transmission, but it is very important in determining the final shape of the beam. Some simulations were run by finding the top transmission by changing the first quadrupole magnet field. When this value was found, other simulations were run with the first quadrupole field fixed and changing the second one to properly shape the beam.

4 Discussion

Top transmission configurations are shown in Table 3. We can observe that the maximum transmission values obtained with each charge compensation value do not significantly change from one layout to another. Moreover, there is not a layout with higher transmission with the three charge compensation values. Therefore, transmission will not be the key factor when deciding which layout we are going to use.

It can also be seen that the transmission is affected significantly by the charge compensation. Transmission is much lower with lower charge compensation values. Therefore, we will target a high charge compensation in the experiment.

One of the most important things that can be observed is that the charge compensation changes not only the transmission but also the optimal field values. For same layouts but different charge compensation values, the optimal magnetic fields can change a lot and we cannot find a direct mathematical correlation between the magnetic fields and the charge compensation through the different layouts. This means that, as we will not know the exact charge compensation value, we will need to be able to vary the fields easily and find the optimal ones during the experiment itself.

If we now look at the Figures 6, 7 and 9, we can observe the final shape of each beam. These figures show the optimal results obtained for each layout with a 0.5 charge compensation. Results for other charge compensations can be consulted in the Appendix. It can be easily seen in Figure 6 - and Figures 12 and 14 - that dq models do not have a good final shape. Looking at either the final *XX'* space phase or at the *Average Envelopes* plots of the figures, we can observe how the beam is divergent. This happened not only with the best result (Fig. 6), but also with all other results. In fact, there is always at least one divergent component when using just one quadrupole magnet because, as shown in Figure 5, while they focus one dimension, the opposite occurs on the other.

All defects explained in the dq case can also be observed in the dqq one. Moreover, one dimension of the dqq beam is divergent and the other is convergent, what means that the shape will evolve from a circular shape- to a planar one. This will cause most particles to get lost through the divergent dimension. Some results with better shape, not converging nor diverging, were also obtained (Fig. 8). However, they have not been presented as the best results due to the loss in transmission compared to the top ones (4.3%).

In the qdq case, it has been possible to find a high transmission result with a good shape. This is because, as explained in Section 2.2, once a field of the first quadrupole magnet has been found to optimize the transmission, the second field has been modified to give it a good shape without affecting the transmission. This cannot be done in the other cases because, in the other cases, all the quadrupole fields affect both the transmission and the shape of the beam.

After analyzing the results, we have decided that the qdq layout will be used for the experiment. The transmission values are very similar for all layouts. Instead, the shape has been a relevant factor, and this layout has shown the best shapes. However, the key factor has been the ease in finding the appropriate field values. In fact, there were some dqq results with good shapes, but it is much more difficult to find the optimal magnetic fields. This factor

is very important because, as explained before, charge compensation has widespread effects and different optimal fields for each case, and we cannot know which is the exact charge compensation value we will face during the experiment. Therefore, the ability to easily find optimal fields for a situation will be essential.

5 Conclusions

As the MIST has to be tested and optimized to work with the IsoDAR for the sterile neutrinos research, we have designed an experiment to measure the produced H_2^+ .

From the three layouts proposed initially, we are going to use the quadrupole-dipole-quadrupole one for our experiment, as it has proven to be the most adaptable layout.

The fields which we will apply to the quadrupole magnets depend on the space charge compensation of the LEBT, which we cannot know. Therefore, we will first adjust the first quadrupole magnetic field to get the optimal transmission and, once this has been accomplished, the second field will be adjusted to obtain a better beam shape.

As we do not know the space charge compensation value, we cannot accurately predict the transmission of the LEBT. However, we expect the space charge compensation to be between 0.5 and 0.8, so we can expect a transmission between 68.4% and 99.0%.

With this information we will be able to build the LEBT and measure MIST's efficiency, so it can be used in the IsoDAR experiment.

6 Future Work

Our most immediate future work will consist in building the LEBT with the information explained in this paper to measure the MIST efficiency. A 3D model of the quadrupole-dipole-quadrupole layout has been created already, as can be seen in Figure 10.

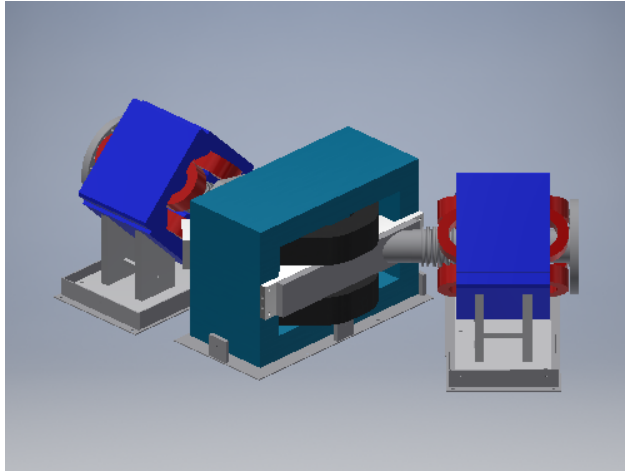


Figure 10: 3D model of one possible arrangement of the LEBT with the dipole magnet between two quadrupole magnets.

Current measurements will be performed with two emittance scanners (Fig. 11). A voltage is applied across these scanners to bend the particles entering and the current is measured with a Faraday cup. The path to the Faraday cup is very narrow, so only the particles following a specific bend can reach it and be measured. Therefore, by changing the voltage applied we can discern the velocity of the particles from their bend. By moving the emittance scanners, one in the vertical direction and the other in the horizontal one, we can determine which ions are coming from the ion source and how the extraction system is shaping and accelerating the beam.

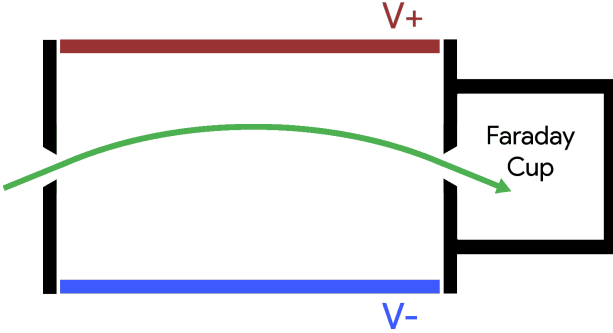


Figure 11: Working diagram of an emittance scanner. The green arrow represents the path followed by the particles measured. Red and blue colors represent the positive and negative voltages applied.

Once MIST is optimized using the experiment we have designed, other components of the whole IsoDAR experiments will be built and improved until it is able to run along KamLAND. We want to run it for 5 years to gather enough data to prove the sterile neutrino's existence.

7 Acknowledgments

First of all, I would like to thank my mentor Joseph Smolsky and all the IsoDAR team at MIT. He has guided me along all this project. His help has been essential for both the research and the paper creation. Secondly, I would like to acknowledge Aina Martínez Zurita, who has been an excellent academic tutor. Her advice was a key factor in the writing process of this paper. Sidhika Balachandar, Blaid Davis, Jenny Sendova and Syamantac Payra have been very helpful by proofreading the paper and suggesting some changes. I also want to thank Loyd Waites, who worked on the MIST's extraction system simulations and gave us

the data required to develop this project. I want to thank my parents, Román and Susana, for supporting and helping me with all my projects and Xavi Bustins for motivating me in the very beginning. I would like to thank the Massachusetts Institute of Technology, the Center for Excellence in Education and the Research Science Institute for giving this amazing opportunity. Finally, I would like to recognize my sponsor: Joves i Ciència from Fundació Catalunya-La Pedrera for making all this possible and also for introducing me to science research.

References

- [1] A. Strumia. Interpreting the lsnd anomaly: sterile neutrinos or cpt-violation or...? *Physics Letters B*, 539(1-2):91–101, 2002.
- [2] J. Formaggio and J. Barrett. Resolving the reactor neutrino anomaly with the katrin neutrino experiment. *Physics Letters B*, 706(1):68–71, 2011.
- [3] C. Dib, J. C. Helo, M. Hirsch, S. Kovalenko, and I. Schmidt. Heavy sterile neutrinos in tau decays and the miniboone anomaly. *Physical Review D*, 85(1):011301, 2012.
- [4] M. Abs, A. Adelmann, J. Alonso, S. Axani, W. Barletta, R. Barlow, L. Bartoszek, A. Bungau, L. Calabretta, A. Calanna, et al. Isodar@ kamland: a conceptual design report for the technical facility. *arXiv preprint arXiv:1511.05130*, page 11, 2015.
- [5] K. Ehlers and K. Leung. High-concentration h2+ or d2+ ion source. *Review of Scientific Instruments*, 54(6):677–680, 1983.
- [6] WARP home. <http://warp.lbl.gov/>. Accessed: 2018-07-20.
- [7] IBSimu ion beam simulator. <http://ibsimu.sourceforge.net/>. Accessed: 2018-07-20.
- [8] E. W. Weisstein. ”Root-Mean-Square” from MathWorld—A Wolfram Web Resource. <http://mathworld.wolfram.com/Root-Mean-Square.html>. Accessed: 2018-07-25.

Appendix A Result Figures

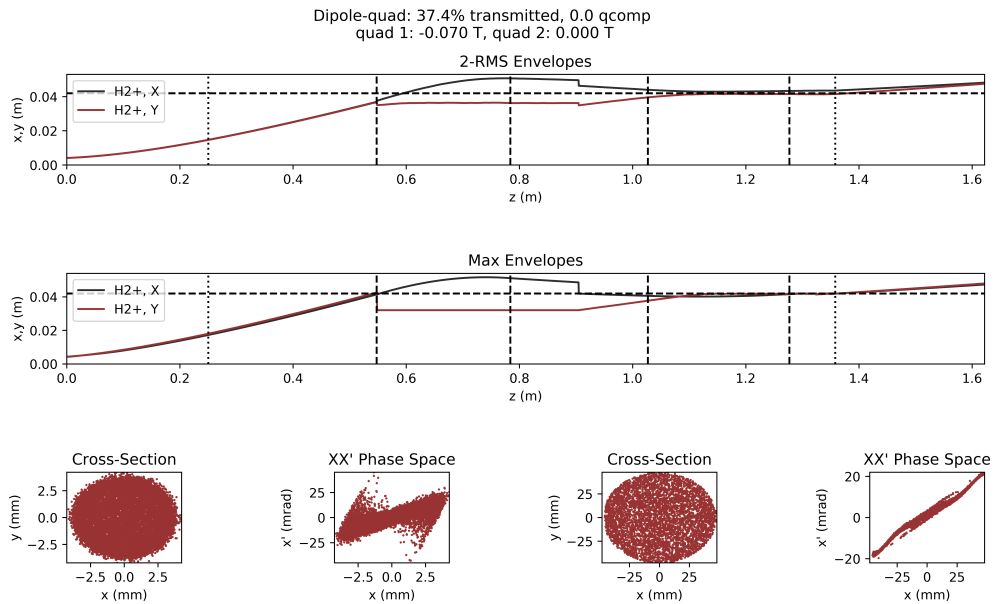


Figure 12: Top transmission result obtained from the dq simulations with charge compensation of 0.

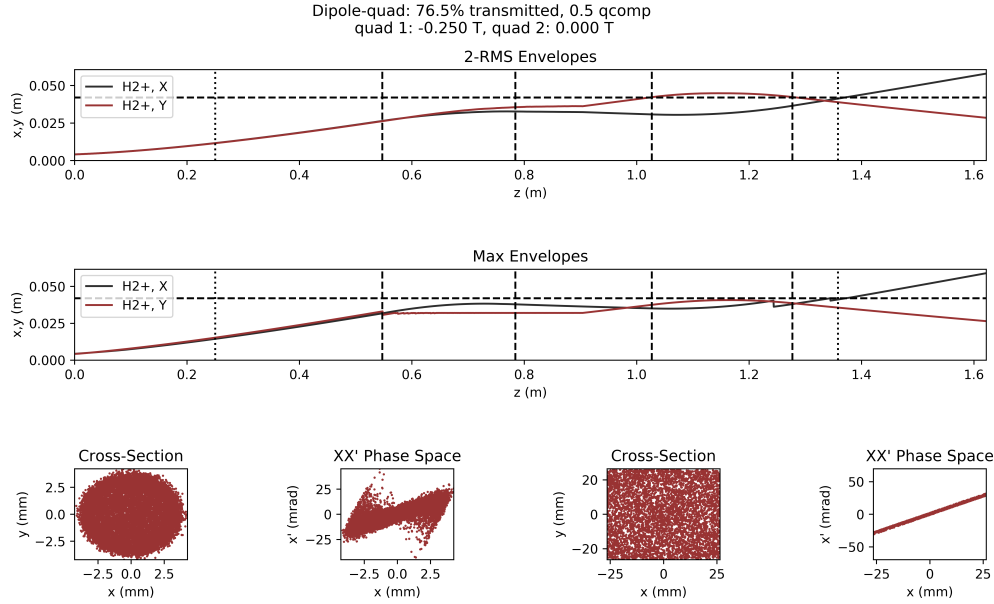


Figure 13: Top transmission result obtained from the dq simulations with charge compensation of 5.

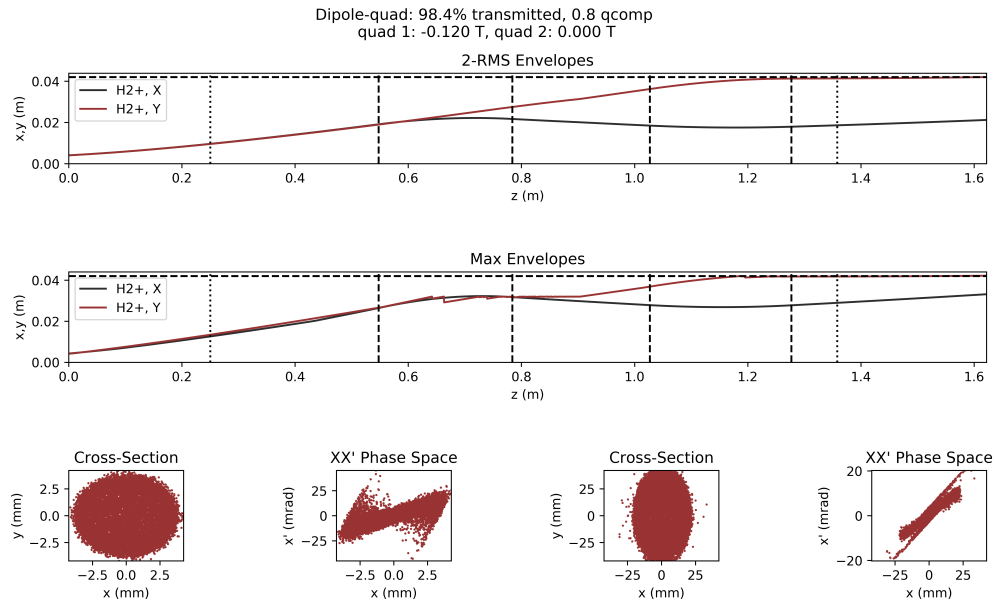


Figure 14: Top transmission result obtained from the dq simulations with charge compensation of 8.

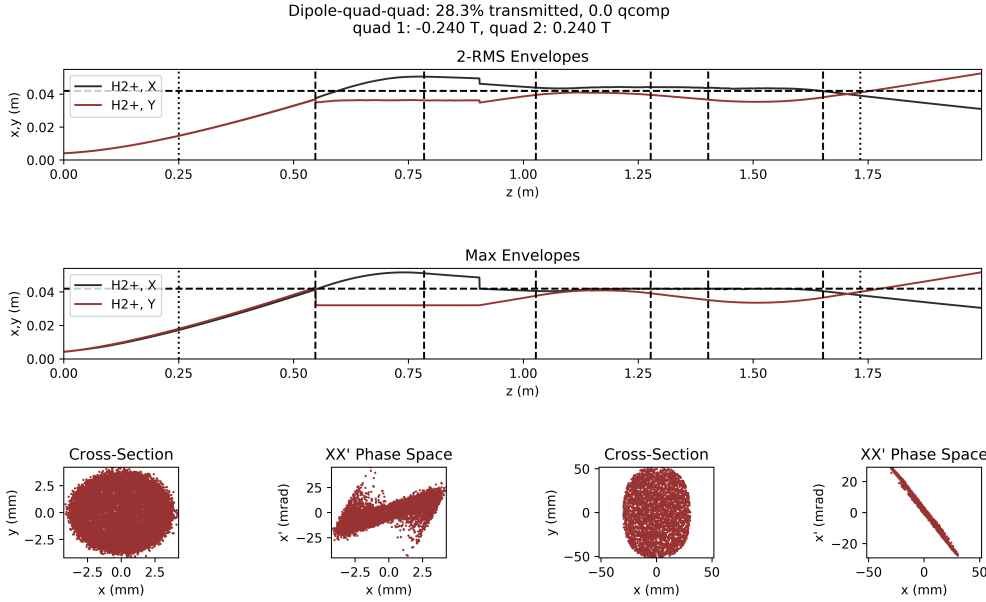


Figure 15: Top transmission result obtained from the dqq simulations with charge compensation of 0.

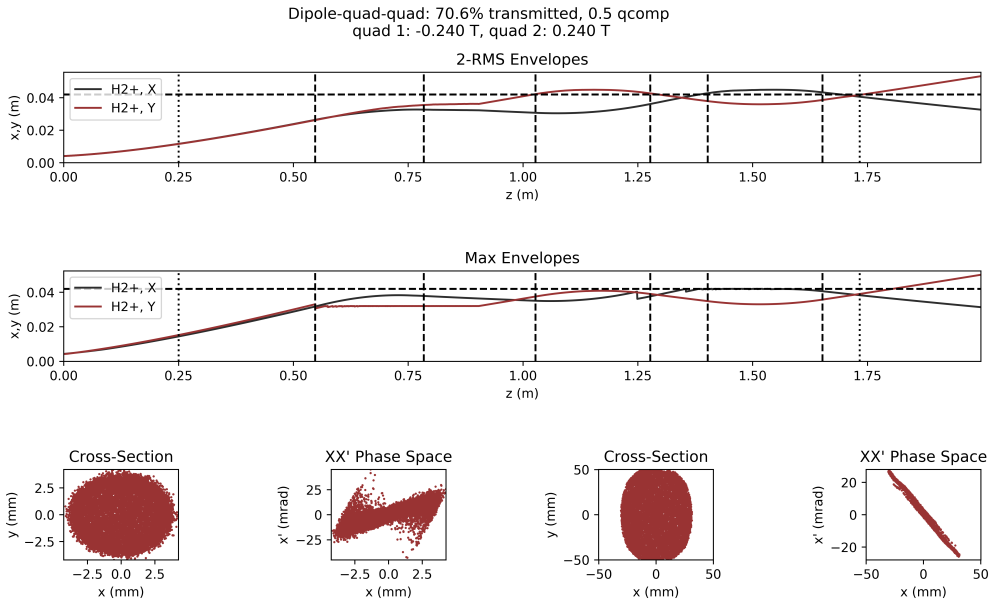


Figure 16: Top transmission result obtained from the dqq simulations with charge compensation of 5.

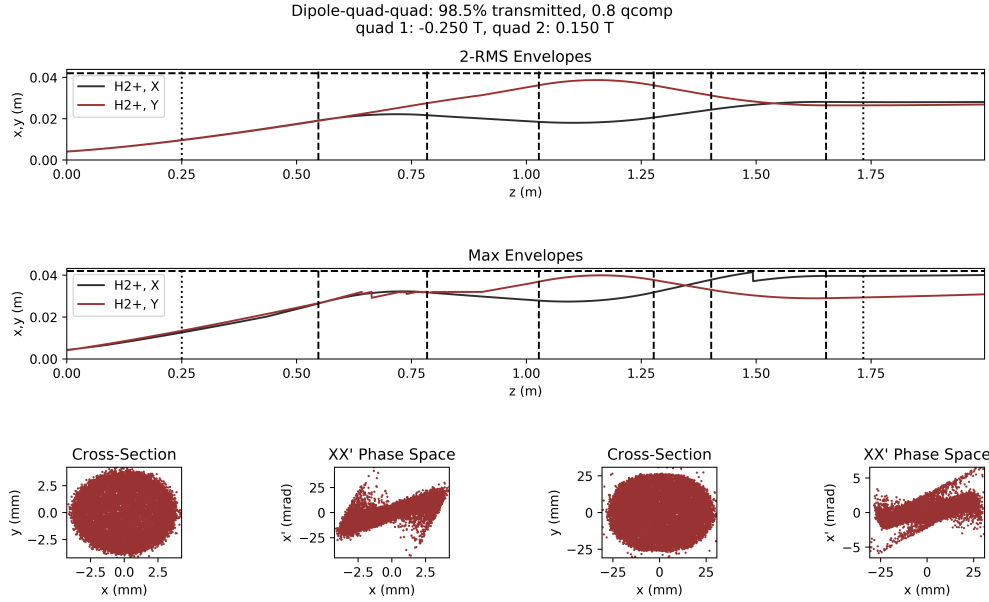


Figure 17: Top transmission result obtained from the dqq simulations with charge compensation of 8.

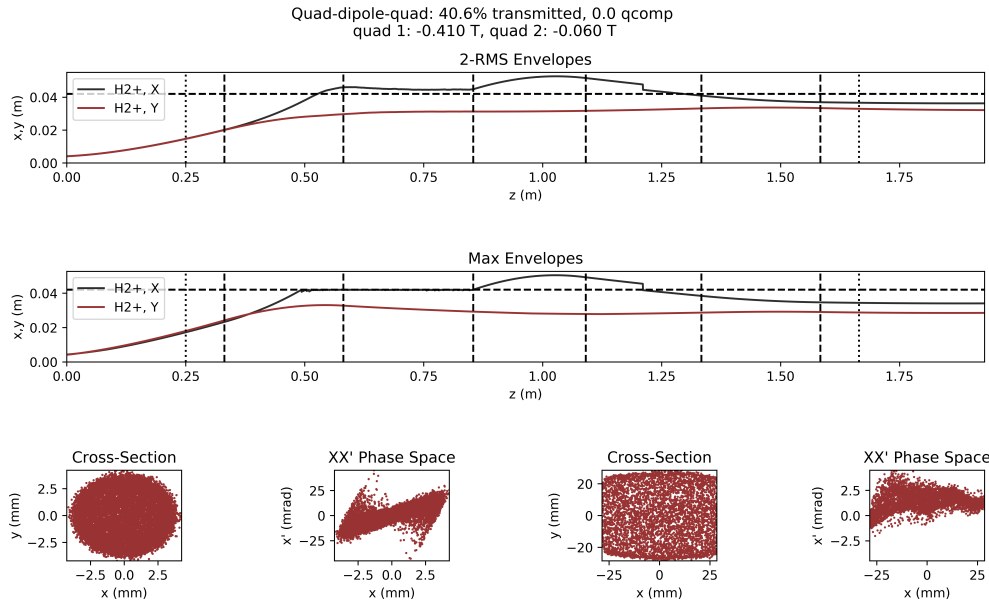


Figure 18: Top transmission result obtained from the qdq simulations with charge compensation of 0.

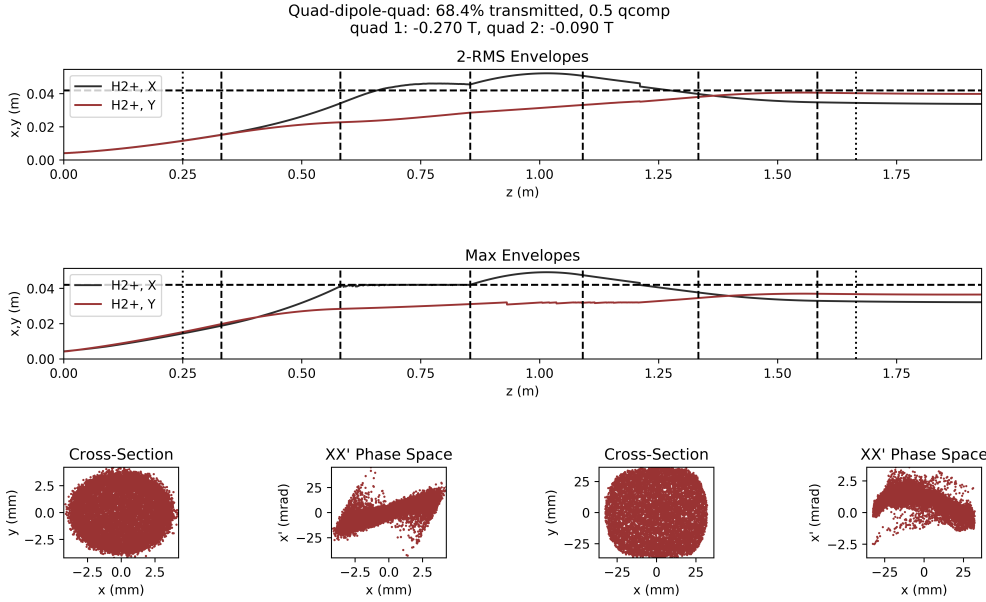


Figure 19: Top transmission result obtained from the qdq simulations with charge compensation of 5.

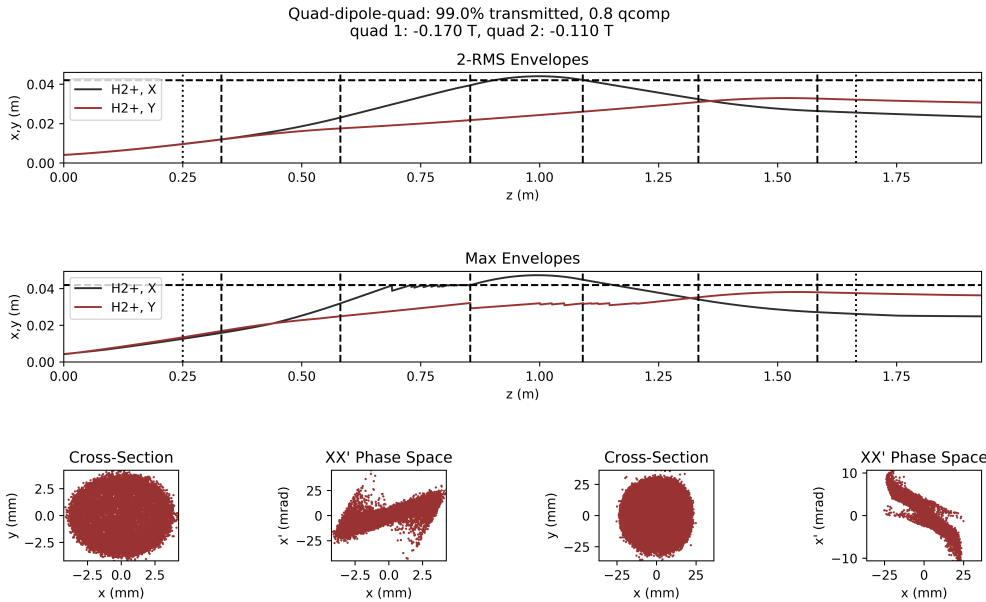


Figure 20: Top transmission result obtained from the qdq simulations with charge compensation of 8.